RSC Advances

ROYAL SOCIETY OF CHEMISTRY

www.rsc.org/advances

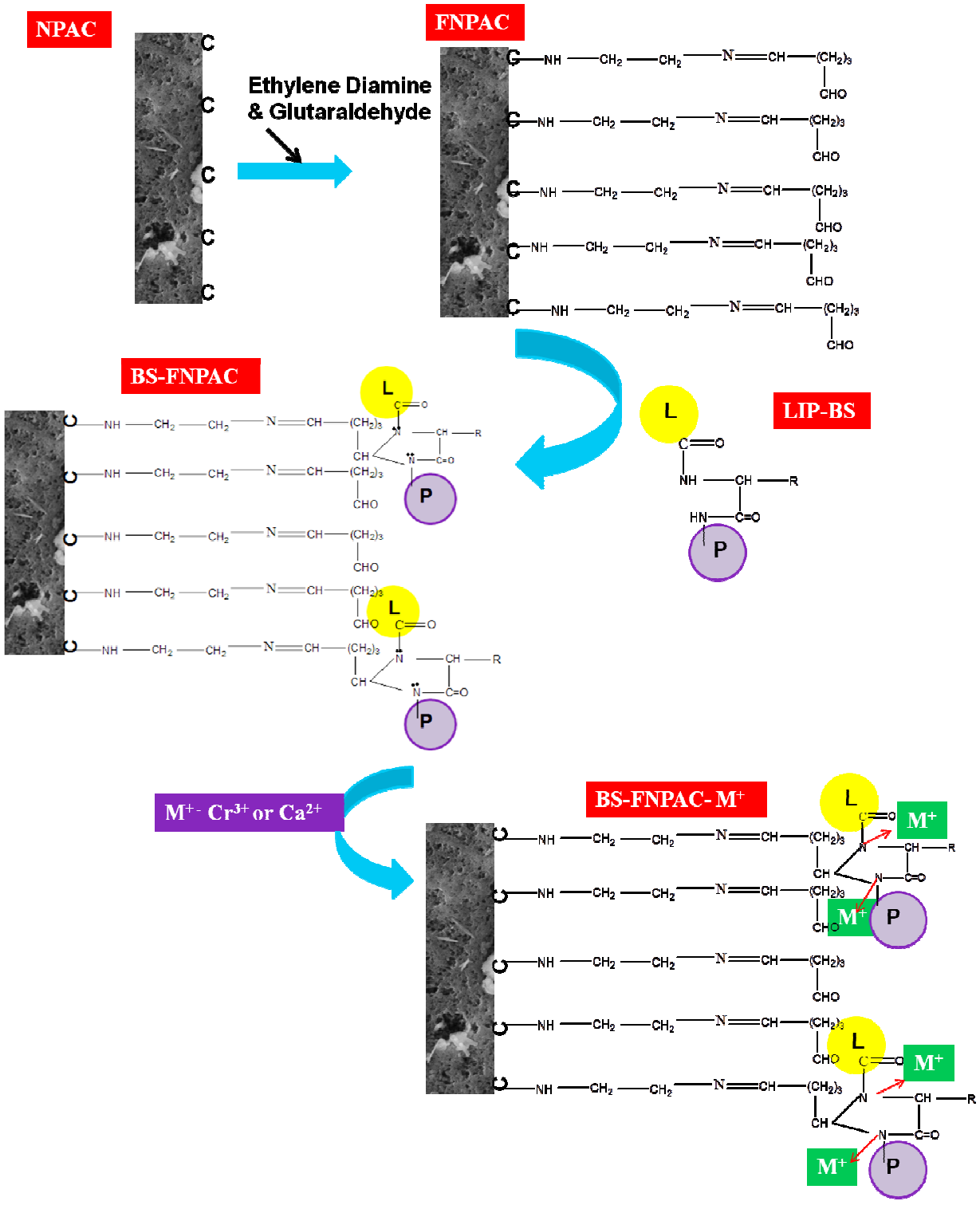

Lipoprotein Biosurfactant from extreme acidophile using fish oil and its immobilization in Nanoporous activated carbon for removal of Metal ions

Lipoprotein biosurfactant production from extreme acidophile using fish oil and its immobilization in Nanoporous activated carbon for the removal of Ca^{2+} and Cr^{3+} in aqueous solution

P.Saranya, S.Swarnalatha and G.Sekaran*

Environmental Technology Division, Council of Scientific and Industrial Research (CSIR)-Central Leather Research Institute (CLRI), Adyar, Chennai- 600 020, Tamilnadu, India.

*** Corresponding Author:**

Tel: +91-44-24452941

Fax: +91-44-24410232

E-mail address: ganesansekaran@gmail.com (Dr. G. Sekaran)

Abstract

The lipoprotein biosurfactant was produced from lipid layer collected from fish processing wastewater (LLFWW) and was immobilized in functionalized nanoporous activated carbon (FNPAC) for sequestering the metal ions (Ca^{2+} and Cr^{3+}) from aqueous solution. The maximum bio transformation of LLFWW into biosurfactant occurred in 96 h in fermentation process using acidophile, *Bacillus subtilis.* The mass of lipoprotein biosurfactant produced was 2.0 g/7.0 g of LLFWW. The lipoprotein biosurfactant was immobilized in FNPAC and the immobilized capacity was 100 mg/g of FNPAC. The biosurfactant immobilized FNPAC removed Cr^{3+} and Ca^{2+} from aqueous solution by 98.24% and 91.76 % respectively. The morphology and functional group characteristics of lipoprotein biosurfactant bound metal ions were determined using scanning electron microscopy (SEM) and Fourier transform infrared spectroscopy (FT-IR) respectively. The sequestrated Ca^{2+} and Cr^{3+} in the FNPAC matrix was confirmed using EPR spectroscopy. The kinetic models for the sequestration of Cr^{3+} and Ca^{2+} by lipoprotein immobilized FNPAC were developed.

Keywords: lipid layer, fish processing wastewater, Lipoprotein biosurfactant, *Bacillus subtilis*, sequestrated of metal ions, Nanoporous activated carbon.

1. Introduction

Recent industrial practices have led to an enormous generation of various crude fatty materials as solid and liquid wastes, which are difficult to treat and valorize.[1] Environmental pollution due to oil & grease containing wastewater is one of the major problems confronting industrial sector across the world. The need to remediate oil laden wastewater has led to the development of new technologies that emphasize on the detoxification and destruction of the contaminants.

Biosurfactants, surface active agents, are produced by certain microorganisms in their growth phase.[2] They may be extracellular or intracellular in nature. They are amphiphilic, non-toxic and biodegradable molecules with high specificity.[2, 3] They have advantages such as low toxicity, higher biodegradability, better environmental compatability, high selectivity, increased specific activity at environmental conditions (extreme temperature, pH, salinity) and the ability to be produced from renewable feedstock.[4] Microbial surfactants are complex molecules, comprising of wide variety of chemical structures such as glycolipids, lipopeptides, fatty acids, polysaccharides-protein complexes, peptides, phospholipids and neutral lipids.[5] These molecules have ability to decrease surface tension, critical micelle concentration and interfacial tension.[6]

Carbon substrate is an important limiting factor affecting the production of microbial surfactants. The type of carbon substrate used for production of biosurfactants has been reported to influence both their quality and yield.[7]

A majority of bacterial biosurfactants have been reviewed extensively on their production, structures and properties[8, 9] using *Bacillus cereus*, [10] *Bacillus pumilus*[11] and *Bacillus polymyxa*[12] and *B.licheniformis*.[13, 14] Amongst bacteria, many *Bacillus* species produce a lipopeptide biosurfactants; the most important one is surfactin which is produced from *Bacillus*

subtilis.[15, 16] It yields better oil recovery due to the reduction of oil viscosity and the interfacial tension.[17] It is advantageous to use biosurfactants in their immobilized form for practical and economical reasons. However, there has been no report on the immobilization of biosurfactant in nanoporous activated carbon (NPAC).

The uninterrupted industrial growth across the globe has resulted in unorganized density of many products on soil and thus contamination of groundwater was the evidence. According to Sparks,[18] there are several types of contaminants that include inorganic species such as nitrate, phosphate, chloride, sulphide, heavy metals (cadmium, chromium, mercury and lead), organic compounds (hydrophobic compounds), and radionuclides.

The wetting agents used in leather processing such as physico- chemical, secondary and tertiary treatment processes can be present in the treated tannery wastewater. The residual unaltered wetting agents foul the ultrafiltration membranes in association with the calcium salts in the wastewater. It has also been proven that calcium can act as a fouling facilitator via a bridging mechanism, enhancing adsorption and complexation with humic acid and the membrane functional groups.[19] Hence, there has been a constant research to develop a technology to remove metal ions in the treated wastewater.

There have been many reports on the ability of biosurfactants to chelate heavy metals in wastewater and form an insoluble precipitate.[20, 21] However, the application of biosurfactants in the free state for the removal of metal ions in the free state does not ensure the reusability, economic viability and environmental compability. Hence, the biosurfactant needs a suitable matrix for its immobilization and effective recovery of metal ions.

In the present investigation, biosurfactant was produced from *Bacillus subtilis* using lipid layer collected from fish processing wastewater (LLFWW) and the partially purified lipoprotein

biosurfactant was immobilized on functionalized NPAC (FNPAC) for the removal of calcium (Ca^{2+}) and chromium (Cr^{3+}) ions from aqueous solutions. This is the first report on production of lipoprotein biosurfactant (LIP-BS) using LLFWW and its immobilization on FNPAC.

2. Materials and Methods

Biosurfactant producing microbial cultures were isolated from soil in fish processing industry, Chennai. Serial dilution technique using nutrient agar was employed to isolate bacteria from soil. Primary screening of isolated bacteria was carried out by staining techniques and biochemical tests. It was identified as *B. subtilis* by morphological, biochemical, and 16S rDNA sequence analysis. The GenBank accession number for the nucleotide sequence is KC921218.

Bacterial culture was inoculated in nutrient broth with fish oil as substrate and it was incubated at optimized conditions incubation time, 24 h, pH, 1, shaker speed, 120 rpm and temperature, 37ºC. The biosurfactant production conditions such as incubation time, pH, temperature and concentration of the LLFWW were optimized using Response surface Methodology (RSM).

The extraction of biosurfactant from cell-free supernatant was carried out by the method followed by Rivardo et al. [22] The pH of cell free supernatant was adjusted to 2 using 1 N HCl and refrigerated at 4ºC for 24 h. It was then centrifuged at 9000 x g for 10 min at 4ºC and pellet was collected. The biosurfactant from the pellet was extracted three times with ethyl acetate/methanol (4:1) mixture. The extracted organic fraction was evaporated to dryness under vacuum, and chilled acetone was added to recover the partially purified biosurfactant. The purity of the biosurfactant was tested using sodium dodecyl sulfate-polyacrylamide gel electrophoresis (SDS PAGE).[23] The lipid, amino acid, and protein contents of purified biosurfactant were

determined by following the methods of Joseph et al., [24] Chen et al., [25] and Lowry et al., [26] respectively.

The Critical Micelle Concentration (CMC) of the purified LIP-BS was determined by dissolving the LIP-BS of various concentrations (10-500 µg/ml) in distilled water and followed by surface tension determination. The surface tension of each concentration was determined in triplicate. The maximum standard deviation associated with the surface activity m easurements was ± 0.2 mN/m. The CMC of the biosurfactant was estimated from the intercept of the plot of biosurfactant concentration against the absolute value of surface tension.

Emulsification stability (E24) of LIP-BS was determined in accordance with the method followed by Cooper and Goldenberg.[27] Two milliliters of fish oil, olive oil, palm oil, coconut oil and diesel were added to the same amount of the cell free broth, mixed using a vortex mixer for 2 min, and left to stand for 24 h. The E24 index was calculated as given below

$$\text{Emulsification stability (E24), (\%)} = \frac{\text{Height of emulsified layer (mm)}}{\text{Total height of the liquid column (mm)}} \times 100$$

The biosurfactant was hydrolyzed at 100°C for 20 h with 6 N HCl and neutralized with 1 M NaOH. The amino acid composition was analyzed using Agilent 1100 HPLC amino acid analyzer, and the data analysis was performed by using HP chem station.

Fourier transform- infrared spectroscopy (Perkin-Elmer) was used for the investigation of surface functional groups in LIP-BS. The samples with KBr (spectroscopic grade) pellets were prepared in the dimensions diameter, 10 mm and thickness, 1 mm. The samples were scanned in the frequency range of 4000 to 400 cm^{-1}.

Required quantity (8-10 mg) of LIP-BS was loaded in platinum TGA pan and thermogravimetric analysis was carried out from 0°C to 800°C, at a temperature gradient of

10°C/min under pure nitrogen atmosphere. Scans were routinely recorded as duplicates using TGA Universal V4.4A TA instruments.

Required quantity of LIP-BS sample (8-10 mg) was loaded in aluminum DSC pan and DSC gravimetric analysis was carried out from 0°C to 300°C under reduced nitrogen atmosphere, at a temperature gradient of 10°C/ min. Scans were routinely recorded as duplicates using DSC Q200 (V23.10 Build 79).

The NPAC was prepared using the method followed by Ramani et al.[28] consisting of precarbonization and chemical activation using 40 % hydrofluoric acid (22 N) at 800ºC. The FNPAC was prepared using the method as described by Ramani et al.[28]

FNPAC of weight 10 g was mixed with solution containing 1.0 g of LIP-BS at pH 9 and kept in thermostatic (temperature maintained at 37ºC) shaker at 120 rpm for strong immobilization of LIP-BS in FNPAC for overnight. The LIP-BS immobilized FNPAC (BS-FNPAC) was washed with distilled water. The BS-FNPAC was packed in a jacketed glass column of dimensions diameter, 2cm and length, 12 cm.

The BS- FNPAC packed glass column was used for the removal of Ca^{2+} and Cr^{3+} from separate aqueous solutions. The optimum conditions were determined by varying time (1, 2, 3, 4, 5 h), pH (4, 4.5, 5, 5.5, 6, 6.5, 7, 7.5), temperature (20º, 30 º, 40 º, 50 º, 60º C) and concentration of Ca^{2+} and Cr^{3+} (100, 200, 300, 400, 500 ppm). The synthetic aqueous solution containing Ca^{2+} and Cr^{3+} were individually prepared in distilled water. The Ca^{2+} solution was prepared using $CaCl_2.2H_2O$ and Cr^{3+} solution was prepared using $Cr_2(SO_4)_3$. The metal ion containing solutions were applied continuously under upflow mode using a peristaltic pump to the reactor packed with BS-FNPAC. The Ca^{2+} and Cr^{3+} ions after passing through the column were estimated using

160 EDTA titrametric (APHA 3500- Ca B)[29] and colorimetric (APHA 3500-Cr B)[29] methods
161 respectively.

162 The non-linear kinetic models were applied to investigate the kinetic rate constants for
163 the adsorption of metal ions (Ca^{2+} and Cr^{3+}) onto BS-FNPAC. The pseudo first order[30] and
164 pseudo second order[31] models were employed, to determine the kinetic order for the adsorption
165 Ca^{2+} and Cr^{3+} onto BS-FNPAC respectively.

166 $$q_t = q_e\,(1 - exp^{-K_1\,t}) \quad (4)$$

167 $$q_t = \frac{K_2 q_e^2 t}{1 + K_2 q_e t} \quad (5)$$

168 where q_e and q_t are the amount of metal ions adsorbed onto BS-FNPAC (mg/ mg of adsorbent) at
169 equilibrium and at any time (t), K_1 and K_2 are the first and second order rate constants.

170 Fourier transform - infrared spectrophotometer (Perkin-Elmer) was used for the
171 investigation of surface functional groups in FNPAC, BS-FNPAC, BS-FNPAC-Ca^{2+} and BS-
172 FNPAC-Cr^{3+}. The samples with KBr (spectroscopic grade) pellets were prepared with
173 dimensions diameter, 10 mm and thickness, 1 mm. The samples were scanned in the frequency
174 range of 4000 to 400 cm^{-1}.

175 The FNPAC, BS-FNPAC, BS-FNPAC-Ca^{2+} and BS-FNPAC-Cr^{3+} were coated with 120-
176 130 μm gold in argon medium. SEM observations were performed on a scanning device attached
177 to a JEOL JM–5600 electron microscope at 20 kV accelerating voltage with an electron beam of
178 wavelength 5-6 nm.

179 The X-ray energy values of BS-FNPAC, BS-FNPAC-Ca^{2+} and BS-FNPAC-Cr^{3+} obtained
180 from the EDX spectra were compared with known characteristic X-ray energy values to
181 determine the presence of Ca^{2+} and Cr^{3+} in the matrices.

EPR spectra were recorded for FNPAC, BS-FNPAC, BS-FNPAC-Ca^{2+} and BS-FNPAC-Cr^{3+} using Bruker X-band EPR spectrometer with an operating frequency of 9.746 GHz and microwave power set at 3.1 mW. Acquisition was carried out in standard quartz tubes (wilmad Labglass) at room temperature conditions.

3. Results and Discussion

Amongst of the bacterial species isolated from soil in fish processing industry, the microorganism exhibited the maximum biosurfactant yield and surface-active property was screened and used in the study. The 16S rDNA sequencing data showed that the isolated organism was *Bacillus subtilis* (Fig. 1). The nucleotide sequence has been assigned an accession number KC921218 from NCBI Gene bank database. *Bacillus subtilis* is a bacterium grown at extremely acidic pH 1 and at temperature 35°C.

Response Surface Methodology (RSM) using central composite design was employed to determine the optimum levels of the four significant factors that affected biosurfactant yield. The high and low levels with the coded levels for the factors are as shown in Table 1. Based on the regression analysis of the data from Table 2, the effect of four factors on biosurfactant yield was predicted by the second order polynomial function as

$$\text{Biosurfactant(g/ml)} = +20.00 - 1.138*A + 0.46*B + 0.37*C - 0.38*D + 0.44*A*B + 0.56*A*C - 0.94*A*D + 0.19*B*C + 0.44*B*D - 0.94*C*D - 1.68*A^2 - 0.93*B^2 - 1.93*C^2 - 0.55*D^2$$

Where A, B, C, D are time, pH, temperature and LLFWW respectively.

The statistical significance of equation was checked by F test and ANOVA for the second order polynomial model as shown in Table 2. The analysis of factor (F test) showed that, the

second order polynomial model was well adjusted to experimental data and the coefficient of variation (CV) and regression coefficient indicated the degree of precision of the experiment.

In general, higher the value of CV, lower the reliability of the experiment. In the present investigation the lower value of CV (7.58) with a regression coefficient of 0.9518 indicated a better precision and reliability of experiments.[32] Linear and quadratic terms were both significant at 1 % level.

The 3D response surface plots described by the regression model were drawn to illustrate the effects of independent factors and interactive effects of each independent factor on the response factors. And also it showed that optimum conditions required for the maximum production of biosurfactant were time, 96 h; temperature, 35 ºC; pH, 9.0 and LLFWW, 7 g/L; (Fig. 2). Each figure presented the effect of two factors while the other factor was held at the zero level.

At the optimized conditions (time, 96 h; temperature, 35 ºC; pH, 9.0; LLFWW, 7 g/L and the maximum biosurfactant yield was found to be 2.0 g / 7.0 g of LLFWW.

The LIP-BS produced in the present investigation was further confirmed through composition of its constituents and composition of amino acids. The lipid, protein, and amino acid contents of the purified LIP-BS were 81, 54, and 25 mg/g, respectively. The molecular weight of the LIP-BS was found to be 78 KDa (Fig.3).

There are few reports on the production of lipopeptide/lipoprotein biosurfactant from *B.subtilis,* [33] but there is no single report on the production of LIP-BS using LLFWW as substrate. The CMC of the purified biosurfactant was 5.7 µg/ml, and the biosurfactant lowered surface tension of water from 65.4 to 31.0 mN/m. Generally, the surface tension at CMCs of various biosurfactants was reported in the range from 27 to 35 mN/m. [34, 35] Thus, the lipoprotein

reported in this present investigation could be classified under efficient and effective surfactant as per norms illustrated by Kim et al. [34] and Parkinson.[36]

The emulsification index of the biosurfactant was evaluated by determining the emulsifying activity with different hydrocarbons. The biosurfactant exhibited different stabilization properties with the hydrocarbons tested as expressed in terms of emulsification activity. Olive oil exhibited the best emulsifying activity (60±1.4%), followed by fish oil (57±1.4%), palm oil (52±1.2%), coconut oil (36± 1.4%) and Diesel (32 ± 0.9%) (Figure not shown).

The amino acid composition of LIP-BS was analyzed using HPLC as shown in table 3. It was found that the LIP-BS contained polar amino acids by 74.08 %, non polar amino acids by 25.84% and aromatic amino acids were absent. The high polar content of biosurfactant suggests that they are highly hydrophilic in nature.

The FT-IR spectrum of LIP-BS is shown in Fig.4. The peak corresponding to amides at 3428.66 cm^{-1}, CO-N stretching present in glycine may be correlated to 1642.10 cm^{-1} and the N-H bond combined with C-N stretching mode at 1806.24 cm^{-1}. The characteristic stretching frequency of amides in the region 3428.66 cm^{-1} may be attributed to histidine present in biosurfactant. The absorption in the region from 1500 to 1650 cm^{-1} is not normally observed in the FT-IR spectra of rhamnolipid biosurfactants, which differentiates the unique nature of LIP-BS from rhamnolipid.[37-39]

The TGA of LIP-BS (Fig. 5a) showed a weight loss by 4.61% at 158.22°C due to removal of moisture. Thereafter, weight loss by 4.77% occurred at 222.67°C. A drastic decrease in weight by 68.87% was observed over the temperature range from 222.67°C to 528.54°C. At the end of the scan (800°C), the sample retained the fixed mass by16 %, indicating the thermal

resistance of the constituents of LIP-BS. The DTA of lipoprotein biosurfactant showed weight loss of 0.1105%/ºC at 168.77 ºC and 0.7922%/ºC at 433.49ºC.

The DSC of LIP-BS (Fig.5b) showed a sharp thermal transition at 95.44°C with enthalpy of transition 489.8 J/g which is due to volatilisation of components present in LIP-BS.

The functionalization of NPAC was carried out with diamine and aldehyde groups. The carboxyl groups present in NPAC was condensed with ethylenediamine to form aminated NPAC and it was further treated with glutaraldehyde to impart extending aldehyde groups to the carbon matrix. The characterization of NPAC and FNPAC was explained in our previous study. [40] The pore diameter of NPAC was found to be in the range 2-4 nm and the surface area was 832m^2/g. The LIP-BS was covalently bound to FNPAC and thus immobilization of biosurfactant in the matrix was strong enough to prevent dislodging during interaction with aqueous solution. After functionalization, the surface area of FNPAC was found to be 156m^2/g.

The FT-IR spectrum of FNPAC (Fig.6a) showed that the peak corresponds to N-H stretching vibration of secondary amine at 3474.35 cm^{-1}. The significant increase in intensity of the band at 1625.13 cm^{-1} in FNPAC corresponds to C-O stretching vibrations of carboxyl or aldehyde groups. This may be due to the addition of ethylenediamine and glutaraldehyde. This confirms the condensation of ethylenediamine and glutaraldehyde groups with NPAC.

The FT-IR spectrum of BS-FNPAC (Fig. 6b) showed that all the peaks corresponding to the biosurfactant besides peaks in the support matrix. The peak observed at 3428.66 cm^{-1} may be attributed to secondary amine and peptide bond.The stretching mode of the CO-N bond was observed at 1,642.10 cm^{-1}. The C-N stretching mode observed at 1806.24 cm^{-1}may be correlated to secondary amine. The shifting frequency of stretching mode of C-H to 3416.26 cm^{-1} in BS-FNPAC confirms the bonding of BS with FNPAC. The absorption region at 1715.57 cm^{-1} is due

to the carbonyl stretching. These stretching vibrations confirmed that the strong binding of biosurfactant with FNPAC.

The surface morphologies of NPAC and FNPAC are illustrated in Fig 7a and Fig 7b. The SEM images clearly illustrate the NPAC was highly porous in nature. The porous nature was created by the chemical activation using hydrofluoric acid. The SEM image of FNPAC reveals that the NPAC was covered with deposit at outer pore surface area and the chemical deposit was uniform in nature with uniform porosity. This may be regarded as amino-aldehyde (Am-Al) chemical deposit on NPAC surface. The LIP-BS immobilized onto NPAC and FNPAC was about 100 mg/g of FNPAC and 58 mg/g of NPAC respectively. The surface morphology of BS-FNPAC (Fig.7c) represents the biosurfactant molecules were well bound to the carrier matrix upon immobilization.

The adsorption ability of metal ions (Cr^{3+} and Ca^{2+}) by pure NPAC was also studied. It was found that the NPAC could adsorb Cr^{3+} and Ca^{2+} ions by about 28.6% and 27.9% respectively from aqueous solution. The removal of Cr^{3+} and Ca^{2+} ions from aqueous solution by LIP-BS immobilized NPAC (BS-NPAC) was studied at the same experimental conditions. The percentage removal of Cr^{3+} and Ca^{2+} ions from the aqueous solution by BS-NPAC was found to be 45.8% and 32.6% respectively. The poor removal of metal ions by BS-NPAC may be due to the weak bonding of biosurfactant to NPAC.

The BS- FNPAC has been used for the removal of metal ions (Cr^{3+} and Ca^{2+}) and the optimization has been carried out as follows. Fig. 8a shows that, BS-FNPAC could remove Cr^{3+} and Ca^{2+} ions from aqueous solution by 82.8% and 77.5% respectively in 2 h. The percentage removal of metal ions was saturated significantly at 3 h, i.e., Cr^{3+}, 81.5% , Ca^{2+}, 75.6% (Fig.8a). Hence, the optimum time needed for the removal of metal ions was considered to be 3 h. The

results conclude that the immobilized LIP-BS in FNPAC has significant removal capacity for Cr^{3+} and Ca^{2+} ions from aqueous solution. The credible increase in removal capacity of BS-FNPAC is due to its stable configuration and high loading of LIP-BS.

pH played a vital role in the removal of metal ions by BS-FNPAC. The experiment was studied by varying the pH from 4.0 to 7.5 (Fig. 8b). The maximum removal of metal ion was observed at pH 5.0 and the removal efficiency was reduced at pH on either side of 5.0. This may be correlated with charge density of the biosurfactant at different pHs. The maximum percentage removal of Cr^{3+} and Ca^{2+} ions by BS-FNPAC was found to be 95% and 82% at pH 5 (Fig.8b). pH plays a very important role in the adsorption of trivalent chromium because of its influence on the formation of different complex species of Cr^{3+} in solution. It was found that FNPAC was effective for the adsorption of Cr^{3+} in the pH range 4- 6.5. The removal efficiency was decreased above pH 6.5, may be due to the precipitation of Cr^{3+} as $Cr(OH)_3$. The maximum adsorption was observed at pH 5, since at this pH, 90% of the total Cr^{3+} is present in soluble complexes of $Cr(OH)^{2+}$ and $Cr_3(OH)_4^{5+}$.[41]

The effect of initial concentration of metal ions on the removal of them from aqueous solution by BS-FNPAC was determined by varying the metal ion concentrations (100-500 ppm). The BS-FNPAC showed higher removal efficiency for Cr^{3+} ions than Ca^{2+} ions. The maximum adsorption of chromium was found to be 97.5 % at the concentration of 200 ppm (Fig.8c). The results also suggested that the metal ions were removed credibly high at lower concentration and suffered the retarded removal of metal ions at higher concentrations. The maximum adsorption of Ca^{2+} ion by BS-FNPAC was found at 200 ppm concentration with removal efficiency of 86.8% (Fig.8c). The concentration gradient could be a reason for the enhanced removal at 200

ppm while the increase in concentration may result in clogging of the pores and diffusion into pores was retarded resulting in poor removal of metal ions.

The effect of temperature on the removal of metal ions from aqueous solution by BS-FNPAC was determined by varying the temperatures as 20, 35, 45, 50, 60 and 70º C. The removal of Cr^{3+} and Ca^{2+} ions by BS-FNPAC at 50ºC were 98.24% and 91.76 % respectively (Fig.8d).

The adsorption of Cr^{3+} by lipoprotein biosurfactant immobilized FNPAC followed pseudo second order kinetics with rate constant 0.96 L mol^{-1} min^{-1}. The adsorption of Ca^{2+} by lipoprotein immobilized FNPAC followed pseudo first order kinetics with rate constant 0.44 min^{-1}.

The FT-IR spectrum of BS-FNPAC-Cr^{3+} (Fig. 9a) showed the characteristic peak for chromium (620 cm^{-1}) was masked during the binding of Cr^{3+} ions with BS-FNPAC. The stretching band at 3428.66 cm^{-1}, attributed to N-H stretching, is shifted to 3439.03 cm^{-1}. The shift in wavelength to a higher value is the confirmation of stabilized bond (increase in force constant) between Cr^{3+} and N-H stretching in BS-FNPAC. It may be assumed that coordinate bond was established between Cr^{3+} and Nitrogen atoms of peptide linkages in the protein moiety of lipoprotein.

The BS-NPAC-Ca^{2+} was subjected to IR studies in the frequency range of 4000 - 400cm^{-1} to confirm the interaction of Ca^{2+} ions with BS-FNPAC. The FT-IR spectrum of BS-FNPAC-Ca^{2+} (Fig.9b) showed the characteristic peak for calcium (523 cm^{-1}) was masked during the adsorption of calcium onto BS-FNPAC, whereas the stretching band at 3428.03 cm^{-1} , attributed to N-H stretching, is shifted to 3444 cm^{-1}. The shift in frequency to a higher value is the confirmation of stabilized bond between calcium and N-H stretching in BS-FNPAC.

The possible mechanism for removal of metal ions by BS-FNPAC would be adsorption through formation of coordinate bonds established between metal ions and peptide linkages of LIP-BS. The non bonded electrons of nitrogen centres in peptide linkages of LIP-BS are involved in the coordinate bonding with the Cr^{3+} and Ca^{2+} ions. The mechanism could be represented as shown in Fig 10.

The BS- FNPAC showed a higher efficiency in the adsorption of metal ions (Fig.11). The surface morphology of BS-FNPAC-Cr^{3+} and BS-FNPAC-Ca^{2+} showed that the matrices surfaces was loaded with metal ions when compared to BS-FNPAC as shown in Fig.7c. The EDX spectra of BS-FNPAC, BS-FNPAC-Cr^{3+} and BS-FNPAC-Ca^{2+} are shown in Fig. 12. The spectra confirmed the adsorption of metal ions (Cr^{3+} and Ca^{2+}) onto the BS-FNPAC.

The EPR spectra of BS-FNPAC, BS-FNPAC-Cr^{3+} and BS-FNPAC-Ca^{2+} are shown in Fig. 13. The spectra reveal that the metal ions (Cr^{3+} and Ca^{2+}) were bound to the BS-FNPAC. The higher intensity of Cr^{3+} suggests that Cr^{3+} has greater binding affinity to BS- FNPAC than Ca^{2+}. This confirms that the BS-FNPAC adsorbs the metal ions (Cr^{3+} and Ca^{2+}) credibly well from aqueous solutions.

4. Conclusions

This work provides the scope for production of potential LIP-BS from LLFWW using *B.subtilis*. The HPLC analysis confirmed the presence of amino acids in the LIP-BS. The LIP-BS was further characterized by SDS-PAGE and FT-IR studies for molecular weight and functional groups. The LIP-BS was immobilized onto FNPAC and the immobilized matrix (BS-FNPAC) was used for the removal of Ca^{2+} and Cr^{3+} from aqueous solutions. The lipoprotein biosurfactant had higher affinity for the removal of Cr^{3+}ions in aqueous solution than Ca^{2+} ions. The functional groups of metal ions bound to LIP-BS were confirmed through scanning electron

364 microscopy (SEM) and Fourier transform infrared (FT-IR) spectroscopy. The adsorption of Cr^{3+}
365 by BS- FNPAC followed pseudo second order kinetics with rate constant 0.96 L mol^{-1} min^{-1}. The
366 adsorption of Ca^{2+} by BS- FNPAC followed pseudo first order kinetics with rate constant 0.44
367 min^{-1}.The adsorption of metal ions with BS-FNPAC was confirmed using SEM- EDX and EPR
368 spectra.

369 **Acknowledgment**

370 The financial assistance from INDEPTH- BSC0111 (CSIR network project) is highly
371 acknowledged.

372 **References**

373 1. P. Fickers, P.H. Benetti, Y. Wache, A. Marty, S. Mauersberger, M.S.Smit and J.M.
374 Nicaud, FEMS Yeast Res. 2005, 6-7, 527-543.
375 2. J.E. Zajic and C.J. Panchal, Crit. Rev. Microbiol. 1976, 5, 39-66.
376 3. D.G. Cooper and J.E. Zajic, Adv. Appl. Microbiol. 1980, 26, 229-253.
377 4. B. Thanomsub, T. Watcharachaipong, K. Chotelersak, P. Arunrattiyakorn, T. Nitoda and
378 H. Kanzaki, J. appl. Microbiol. 2004, 96, 588-592.
379 5. I.M. Banat, R.S. Makkar and S.S. Cameotra, Appl. Microbiol. Biotechnol. 2000, 53, 495–
380 508.
381 6. I.M. Banat, ACTA Biotechnologica 1995, 15, 251-267.
382 7. P. Das, S. Mukherjee and R. Sen, Bioresour. Technol. 2009, 100, 1015–1019.
383 8. J.D. Desai and I.M. Banat, Microbiol. Mol. Biol. Rev. 1997, 61, 47-64.
384 9. A. Fiechter, Trends Biotechnol. 1992, 10, 208-217.
385 10. M. Nitschke, S.G Costa and J. Contiero, Appl. Biochem. Biotechnol. 2009, 160, 2066–
386 2074.

11. I. Grangemard, J. Wallach, R. Maget-Dana and F. Peypoux, Appl. Biochem. Biotechnol. 2001, 90, 199–210.

12. D. Landman, C. Georgescu, D.A. Martin and J. Quale, Clin. Microbiol. Rev. 2008, 21, 449–465.

13. T. Imura, Y. Masuda and S. Ito, J. Oleo Sci. 2008, 57, 415– 422.

14. S.M.M. Dastgheib, M.A. Amoozegar, E. Elahi, S. Asad and I.M. Banat, Biotechnol. Lett. 2008, 30, 263–270.

15. M. Nitschke and G.M. Pastore, Bioresour. Technol. 2006, 97, 336–341.

16. M. Nitschke and G.M. Pastore, Appl. Biochem. Biotechnol. 2004, 112, 163–172.

17. A. Soudmand-Asli, S.S. Ayatollahi, H. Mohabatkar, M. Zareie and S.F. Shar- iatpanahi, J. Pet. Sci. Eng. 2007, 58, 161–172.

18. D.L. Sparks, Academic Press, San Diego, United States, 1995, pp.267.

19. Qilin, Li and M. Elimelech Environ. Sci. Technol. 2004, 38, 4683-4693.

20. J. Thaniyavarn, A. Chongchin, N. Wanitsuksombut, S. Thaniyavarn, P. Pinphanichakarn, N. Leepipatpiboon, M. Morikawa and S. Kanaya, J. Gen. Appl. Microbiol. 2006, 52, 215–222.

21. C.H.David, F.A. Janick and M.M.Raina, Environ.Sci.Technol. 1995, 29, 2280-2285.

22. F. Rivardo, R.J. Turner, G. Allegrone, H. Ceri and M.G. Martinotti, Appl. Microbiol. Biotechnol. 2009, 83, 541-553.

23. U.K. Laemmli, Nature 1970, 227, 680–685.

24. A.K. Joseph, A. Shauna and M. James, Clin. Chem. 1972, 18, 199-202.

25. L. Chen, Q. Chen, Z. Zhang and X. Wan, J. Food. Comp. and anal. 2009, 22, 137-141.

409 26. O.H. Lowry, N.J. Rosebrough, A.L. Farr and J. Randal, J. Biol. Chem. 1951, 193, 265–
410 275.
411 27. D.G. Cooper and B.G. Goldenberg, Appl. Environ. Microbiol. 1987, 53, 224-229.
412 28. K. Ramani, S. Karthikeyan, R. Boopathy, L. John Kennedy, A.B. Mandal and G.
413 Sekaran, Process Biochem. 2012, 47, 435–445.
414 29. American public health assosciation, Standard methods for the examination of water and
415 waste water, 21st edition, APHA, Washington DC (2005).
416 30. S. Lagergren and B.K. Svenska, Veternskapsakad Handlingar 1898, 24, 1–39.
417 31. Y.S. Ho and G. Mckay, Transl. chem. E 1998, 76B, 183–191.
418 32. G.E.P. Box, W.G. Hunter and J.S. Hunter, Wiley, New York, 1978.
419 33. K.V. Pathak and H.K. Keharia, 3 Biotech 2014, 4, 41–48.
420 34. S.H. Kim, E.J. Lim, S.O. Lee, J.D. Lee and T.H. Lee, Appl. Biochem. Biotechnol. 2000,
421 31, 249-253.
422 35. W.S. Suk, H.J. Son, G. Lee and S.J. Lee, J. Microbiol. Biotechnol. 1999, 9, 56-61.
423 36. M. Parkinson, Biotechnol. Adv. 1985, 3, 65-83.
424 37. C.G. Kumar, S.K. Mamidyala, B. Das, B. Sridhar, G.S. Devi and M.S. Karuna, J.
425 Microbiol. Biotechnol. 2010, 20, 1061-1068.
426 38. N. Christova, B. Tuleva, Z. Lalchev, A. Jordanov and B. Jordanov, Z Naturforsch C
427 2004, 59, 70-74.
428 39. Z. Raza, Z.M. Khalid and I.M. Banat, J. Environ. Sci. Health Part A.2009, 44, 1367-
429 1373.
430 40. P.Saranya, K.Ramani and G.Sekaran, RSC Adv. 2014, 4, 10680-10692.

41. R. Leyva Ramos, L. Fuentes Rubio, R. Guerrero Coronado and J.Mendoza Barron, J. Chem. Tech. Biotechnol. 1995, 62, 64-67.

Figure Captions

Fig. 1. Rooted phylogenetic tree showing the relationship of *Bacillus subtilis* with other closely related species and values shown in the parenthesis are accession number.

Fig.2. Response surface curve for biosurfactant(g) by *B.subtilis* as the function of a). time (h) and pH, b). time (h) and temperature (ºC) and c). time (h) and concentration of substrate (g/L)

Fig.3. SDS-PAGE showing the molecular weight of purified lipoprotein biosurfactant. **Lane 1** molecular weight marker, **lane 2** lipoprotein biosurfactant

Fig.4. FT-IR Spectrum of lipoprotein Biosurfactant

Fig.5. (a) TGA and (b) DSC of lipoprotein biosurfactant

Fig.6. FT-IR spectra of (a) FNPAC and (b) BS immobilized FNPAC

Fig.7. SEM images of a) NPAC b) FNPAC c) BS-FNPAC

Fig.8. (a) Effect of time (h), (b) Effect of pH, (c) Effect of metal ion concentration (ppm) and (d) Effect of temperature, º C on adsorption of Cr^{3+} and Ca^{2+} ions by using BS- FNPAC

Fig.9. FTIR spectra of (a) BS-FNPAC- Ca^{2+} and (b) BS-FNPAC- Cr^{3+}

Fig. 10. Schematic representation of adsorption of metal ions onto the BS-FNPAC

Fig.11. SEM images of (a) Cr^{3+} adsorbed on BS-FNPAC (b) Ca^{2+} adsorbed on BS-FNPAC.

Fig.12. EDX spectra of (a) BS-FNPAC, (b) Cr^{3+} bound BS-FNPAC and (c) Ca^{2+} bound BS-FNPAC.

Fig.13. EPR spectra of FNPAC, BS-FNPAC, Cr^{3+} bound BS-FNPAC and Ca^{2+} bound BS-FNPAC.

Table legends

Table 1. Coded and real values of the factors tested in the RSM experimental design.

Table 2.ANOVA for the second order polynomial model for biosurfactant production.

Table 3. Amino acid composition of lipoprotein biosurfactant

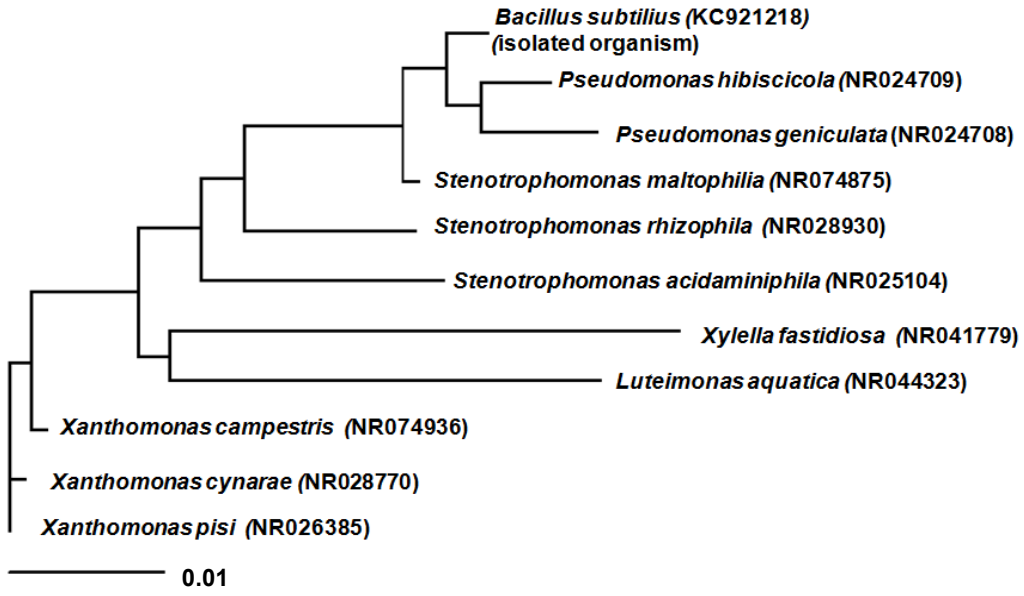

Fig. 1. Rooted phylogenetic tree showing the relationship of *Bacillus subtilis* with other closely related species and values shown in the parenthesis are accession number.

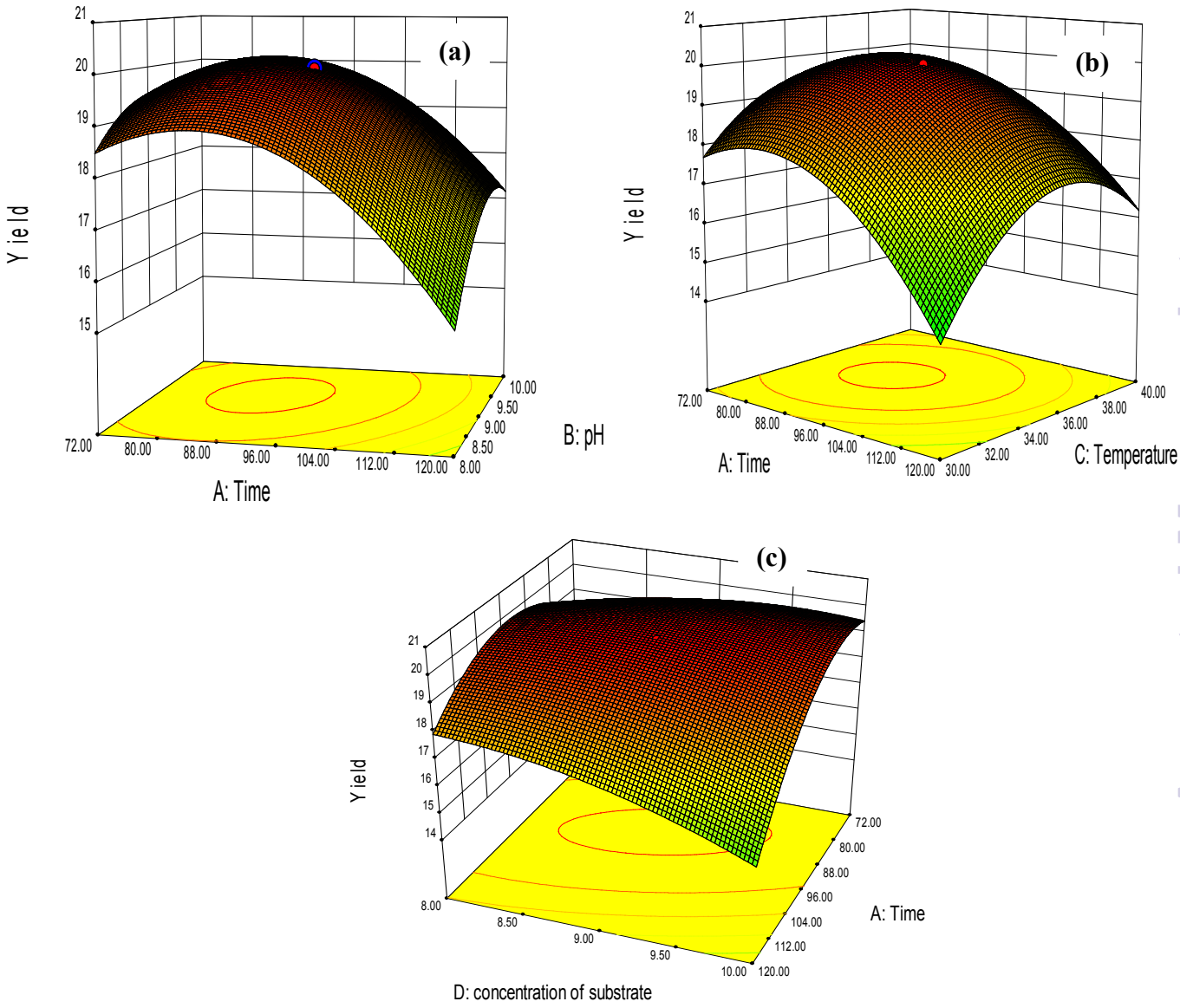

514

515

516

517 **Fig.2.** Response surface curve for biosurfactant (g) by *B.subtilis* as the function of a). time (h)

518 and pH , b). time (h) and temperature (ºC) and c). time (h) and concentration of substrate (g/L)

519

520

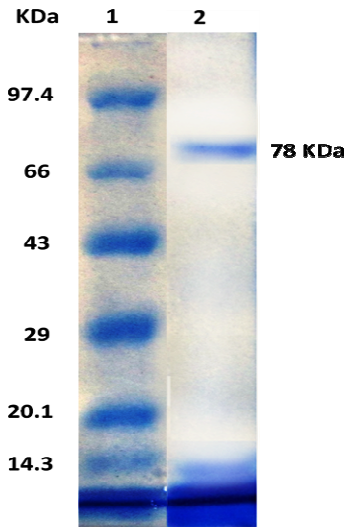

Fig. 3. SDS-PAGE showing the molecular weight of purified lipoprotein biosurfactant. **Lane 1** molecular weight marker, **lane 2** lipoprotein biosurfactant

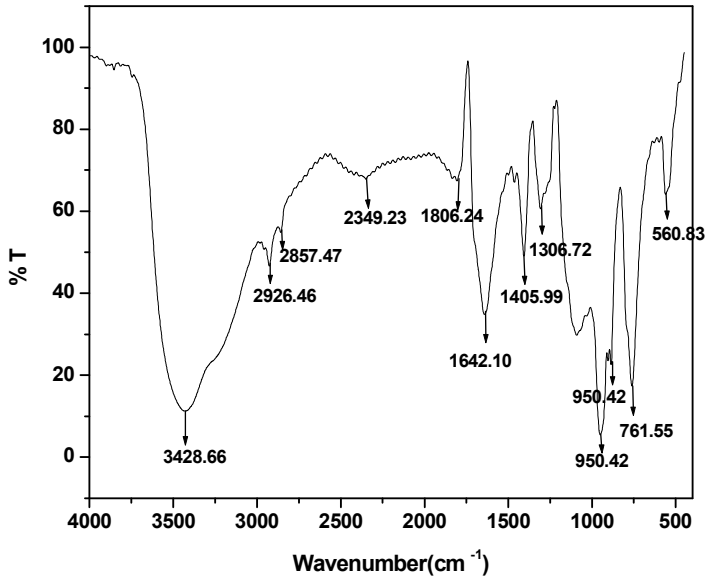

Fig. 4. FT-IR Spectrum of lipoprotein Biosurfactant

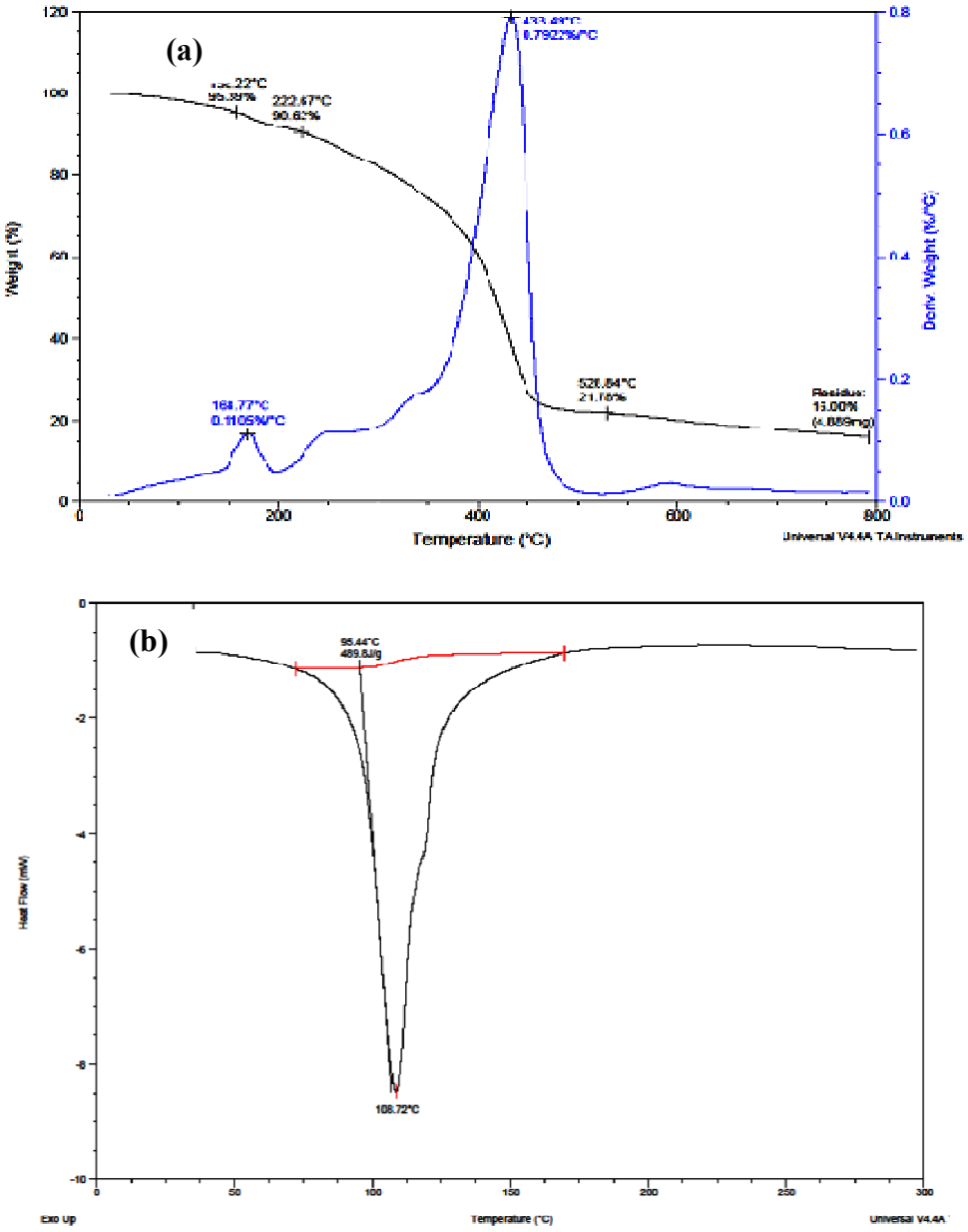

548

549

550 **Fig.5.** (a) TGA and (b) DSC of lipoprotein biosurfactant

551

552

553

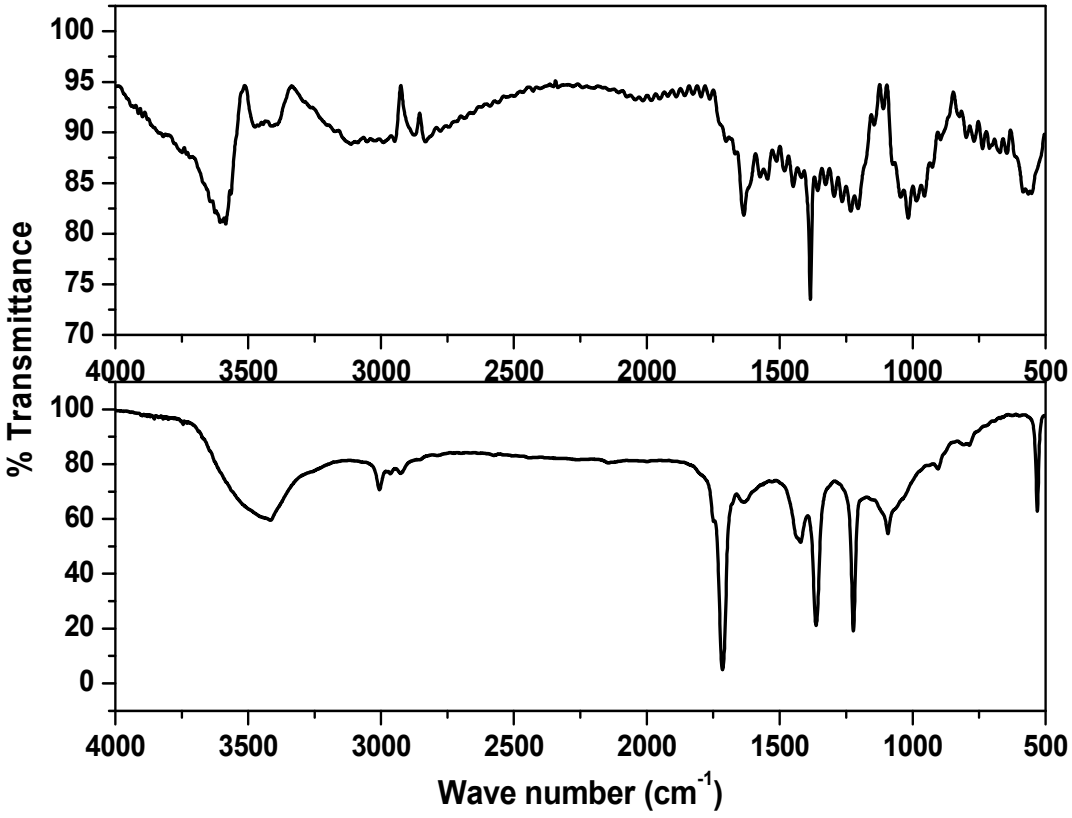

Fig.6. FT-IR spectra of (a) FNPAC and (b) BS immobilized FNPAC

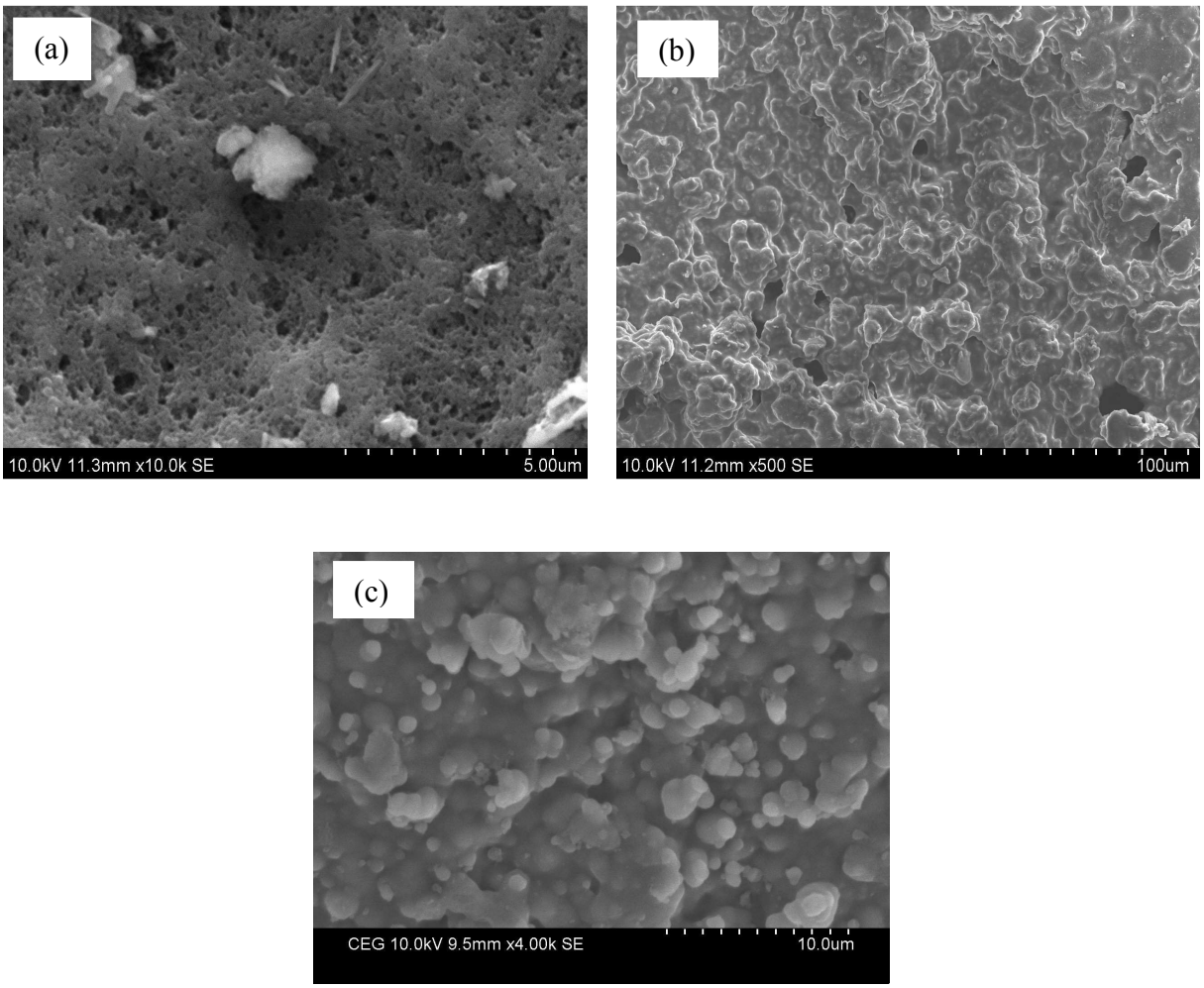

Fig.7. SEM images of a) NPAC b) FNPAC c) BS-FNPAC

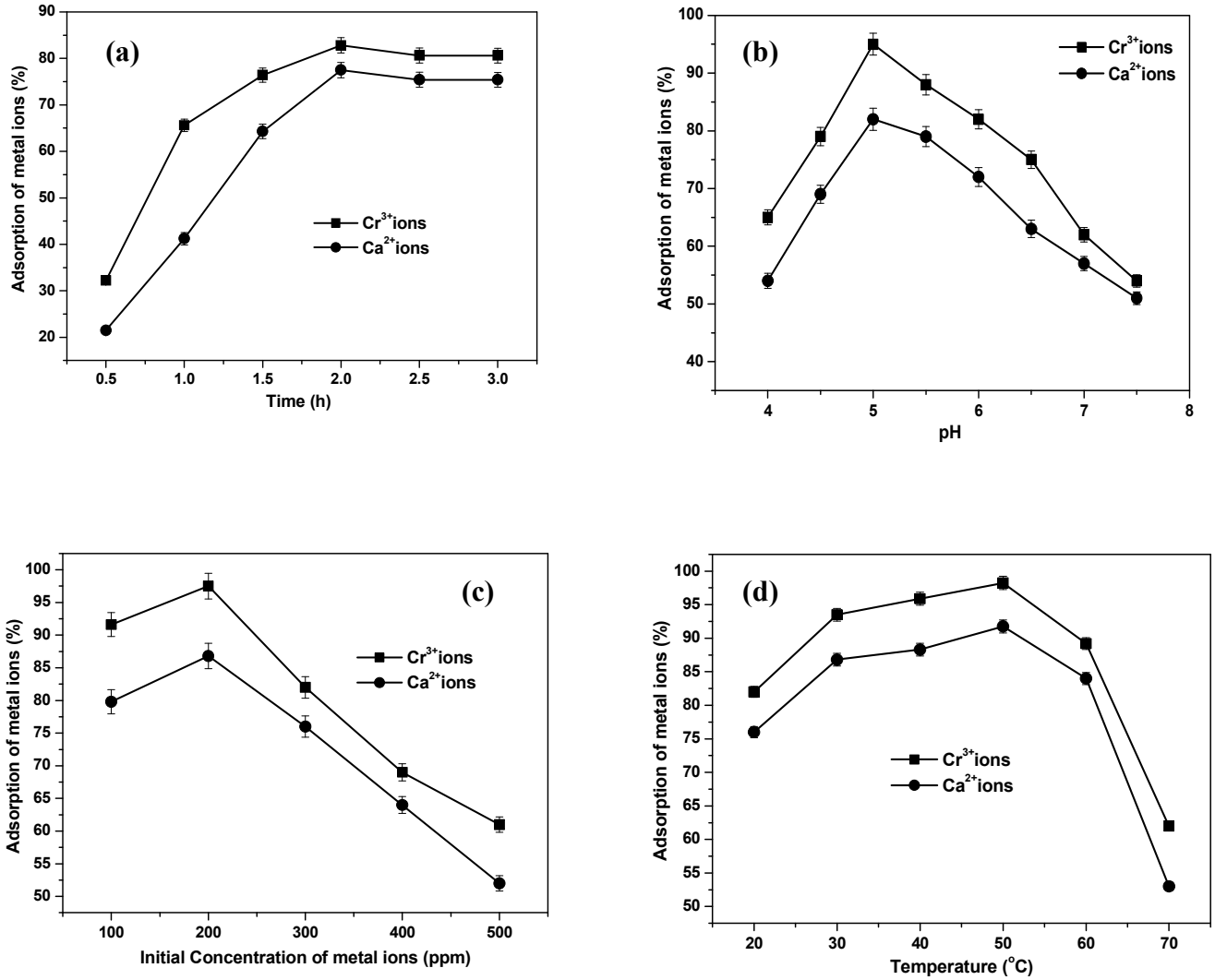

Fig.8. (a) Effect of time (h), (b) Effect of pH, (c) Effect of metal ion concentration (ppm) and (d) Effect of temperature, º C on adsorption of Cr^{3+} and Ca^{2+} ions by using BS- FNPAC

582

583

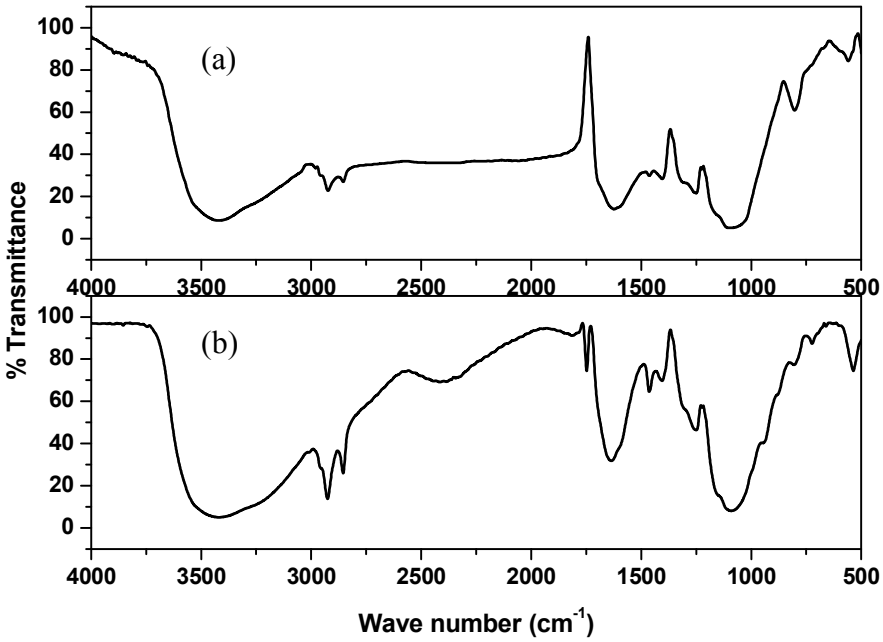

584

585

586

587

588 **Fig.9.** FTIR spectra of (a) BS-FNPAC- Ca^{2+} and (b) BS-FNPAC- Cr^{3+}

589

590

591

592

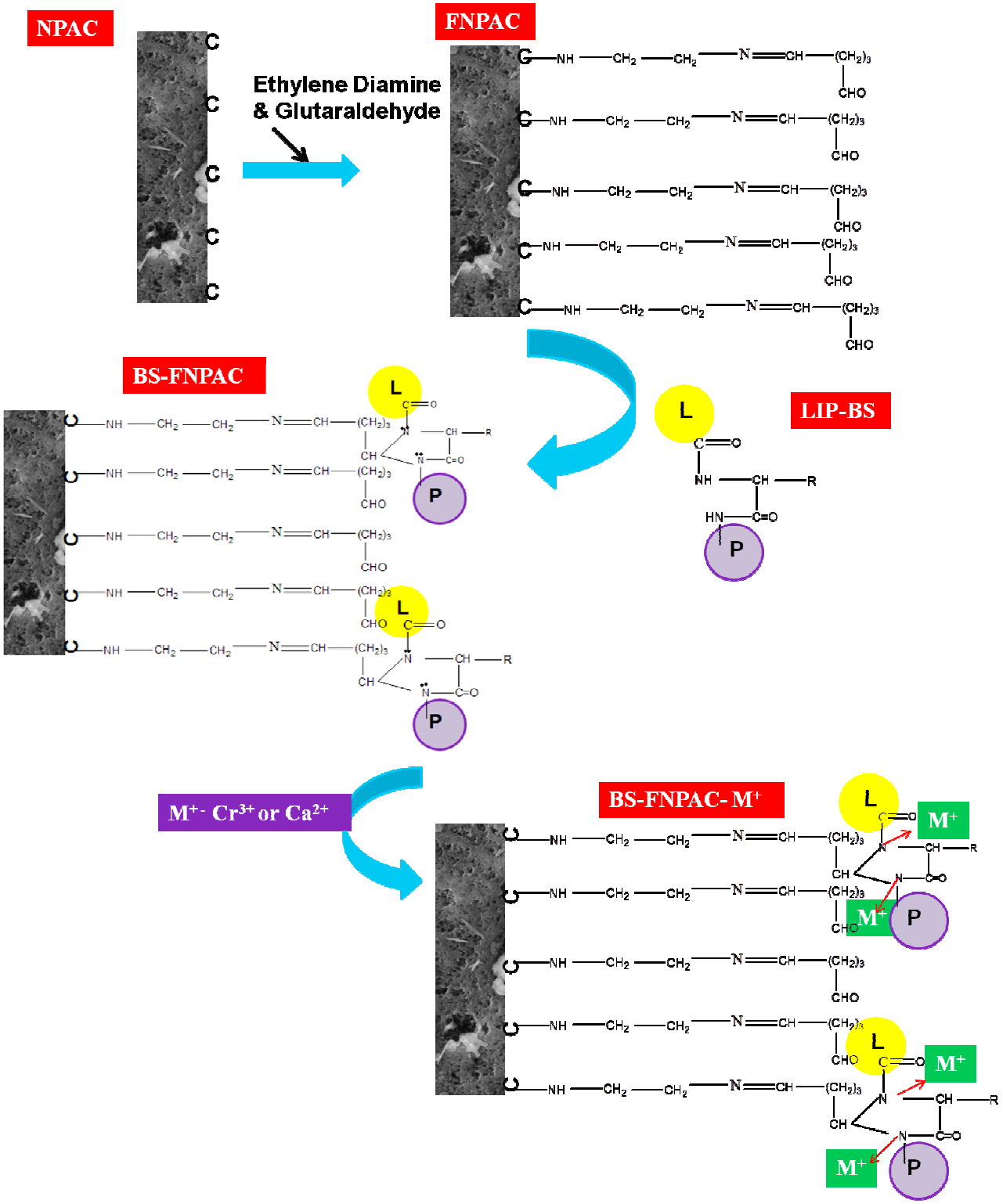

593

594 **Fig.10.** Schematic representation of adsorption of metal ions onto the BS-FNPAC
595 L-Lipid & P- Protein of LIP-BS

596

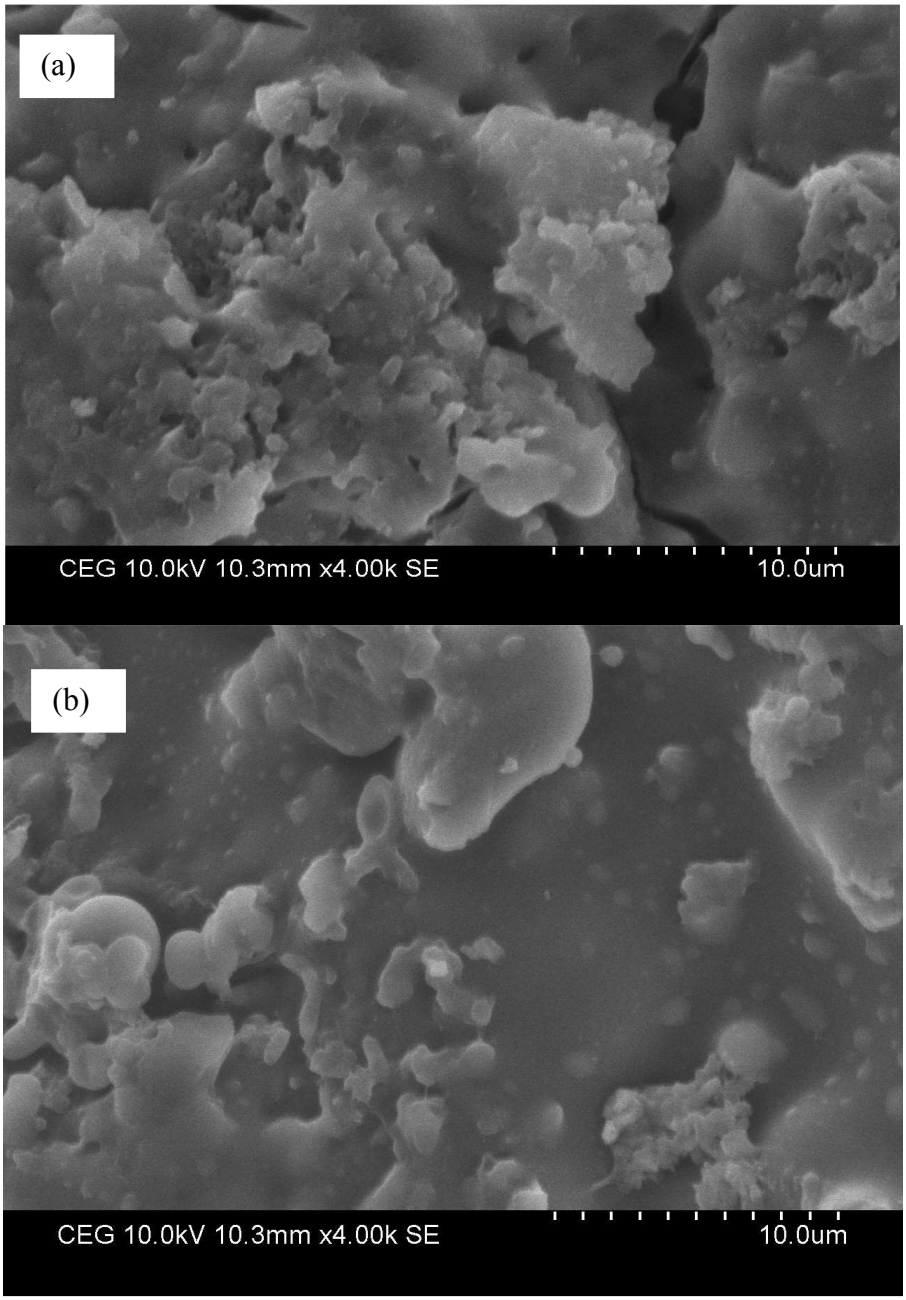

597

598 **Fig.11.** SEM images of (a) Cr^{3+} adsorbed onto BS-FNPAC (b) Ca^{2+} adsorbed onto BS-FNPAC

599

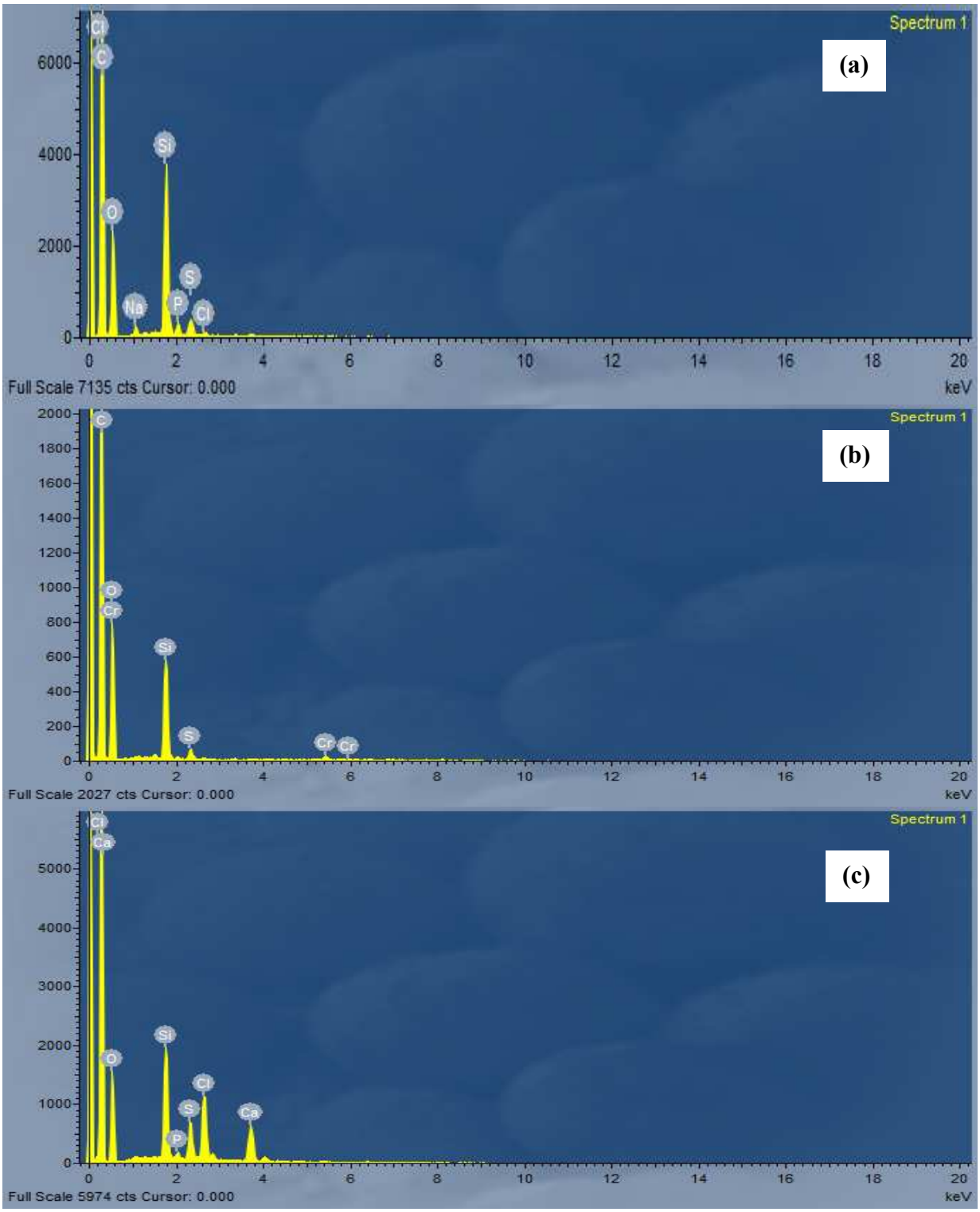

Fig.12. EDX spectra of (a) BS-FNPAC, (b) Cr^{3+} bound BS-FNPAC and (c) Ca^{2+} bound BS-FNPAC

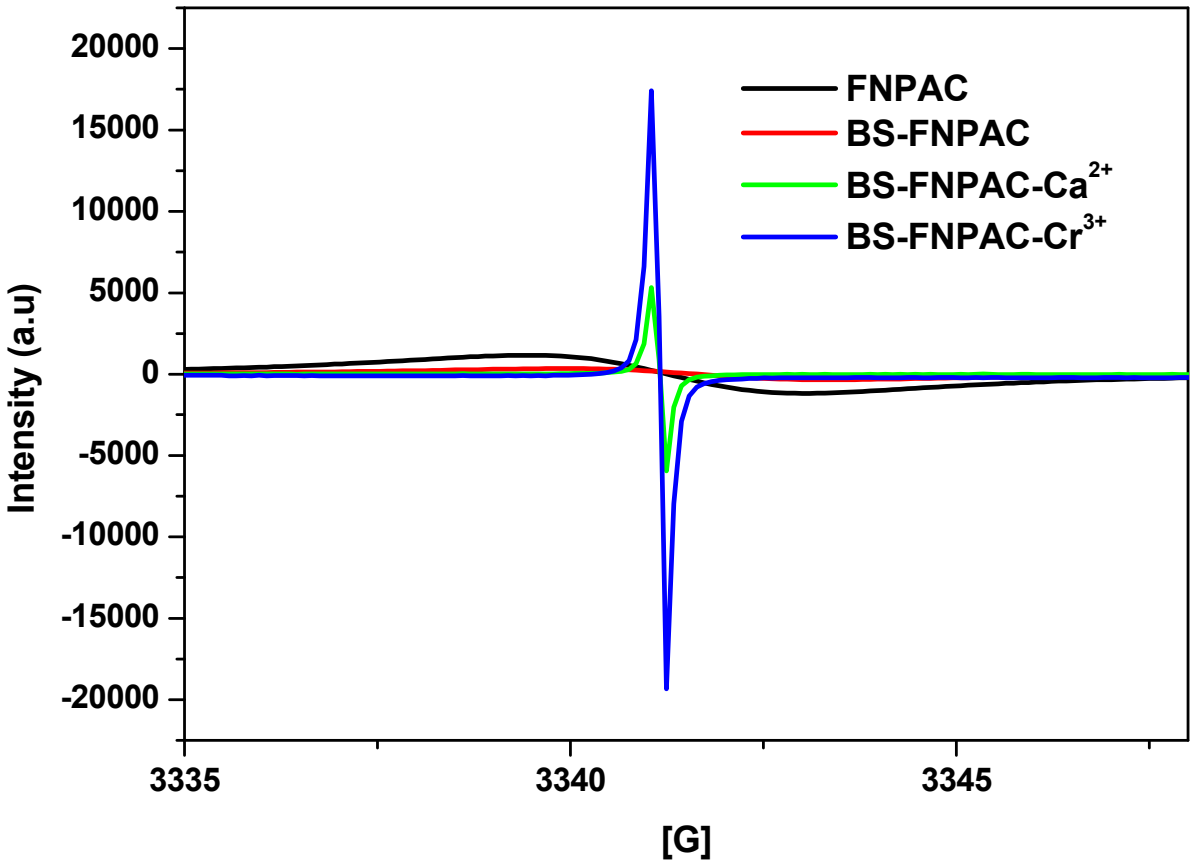

Fig.13. EPR spectra of FNPAC, BS-FNPAC, Cr^{3+} bound BS-FNPAC and Ca^{2+} bound BS-FNPAC

Table 1

Coded and real values of the factors tested in the RSM experimental design.

Factor		Levels of factors	
		-1	**+1**
X1	Concentration of Substrate (ml/L)	8	10
X2	pH	8	10
X3	Temperature (°C)	30	40
X4	Time	72	120

633
634
635
636
637
638
639

640 **Table 2**

641 ANOVA for the second order polynomial model for biosurfactant production

source	**Degree of freedom**	**Mean square**	**F- value**	**P value prob> F**
Model	14	17.53	21.18	<0.0001(significant)
Residual	15	0.83		
Lack of fit	10	1.24		
Pure error	5	0		
Total	29			
R^2				0.9518

642
643
644
645
646
647
648
649

Table 3

Amino acid composition of lipoprotein biosurfactant

S.No	Amino acid	Mol %
1	Arginine	2.32
2	Histidine	9.67
3	Glycine	74.08
4	Serine	8.04
5	Lysine	5.81